ELSEVIER

www.elsevier.nl/locate/ica

Inorganica Chimica Acta 294 (1999) 224–231

Inorganica Chimica Acta

Studies in aryltin chemistry Part XIV. Crystal and molecular structures of tris(*o*-methoxyphenyl)tin(IV) chloride, fluoride and oxide☆

Ivor Wharf *, Anne-Marie Lebuis, Gillian A. Roper

Department of Chemistry, McGill University, Montreal, Québec, Canada H3A 2K6

Received 28 June 1999; accepted 26 July 1999

Abstract

Full crystal structures are reported for the tris(*o*-methoxyphenyl)tin compounds, $(o\text{-}CH_3OC_6H_4)_3SnX$ [X = Cl (**A**), F (**B**)] and $[(o\text{-}CH_3OC_6H_4)_3Sn]_2O$ (**C**), together with both solid-state and solution ($CDCl_3$) ^{119}Sn NMR data for **B** and **C** as well as $(Mes)_3SnF$ and $[(o\text{-}Tol)_3Sn]_2O$. Compound **B** like **A** is monomeric with a similar but not identical arrangement of aryl groups around the tin while NMR data indicate that **B** has almost the same geometry in solution as in the solid state. The anomalously lower frequency $\delta(^{119}Sn)$ value for **B** is consistent with the more ionic character of the Sn–F bond compared with other Sn–X (X = Cl, Br, I) bonds. Compound **C** is the first $(Ar_3Sn)_2O$ with an Sn–O–Sn bond angle between 140 and 180°. The comparison of solid-state with solution $^2J(^{119}Sn,^{119}Sn)$ values for **C** and $[(o\text{-}Tol)_3Sn]_2O$ suggests that the solid state favours structures having larger Sn–O–Sn angles. Reacting **C** with water gives $(o\text{-}CH_3OC_6H_4)_3SnOH$ only in solution, identified by its ^{13}C and ^{119}Sn NMR spectra.

Keywords: Crystal structures; Solid-state/solution ^{119}Sn NMR; Tris(*o*-methoxyphenyl)tin compounds

1. Introduction

The structures of triaryltin compounds, Ar_3SnX (X = Cl, Br, I) that have been reported to date, are almost without exception monomeric having a quasi-tetrahedral geometry at tin [2–4], regardless of the aryl groups present. Only when at least one of the ring substituents itself is a potential donor, does polymer formation occur resulting in a *trans*-C_3SnZY trigonal-bipyramidal geometry at the tin. One example is $[p\text{-}MeS(O_2)C_6H_4]_3SnCl$ where the *para*-methylsulfonylphenyl group acts as a bridge giving an intermolecular organotin–sulfone adduct with the weak Sn–O interaction stabilised in the solid state by polymer formation [2]. In contrast, structures of triaryltin fluorides and hydroxides are dependent on the steric requirements of the aryl groups around the central tin atom, being either polymeric (Ar = Ph; X = F [5] or OH [6]) or monomeric (Ar = 2,4,6-$Me_3C_6H_2$; X = F or OH [7]). Previously we have used *o*-anisyl (*o*-methoxyphenyl) as a sterically demanding aryl group to prepare the monomeric $(o\text{-}MeOC_6H_4)_3SnNCS$ for comparison with polymeric Ph_3SnNCS [8–10] and $(p\text{-}Tol)_3SnNCS$ [8]. We now report an analogous study of $(o\text{-}MeOC_6H_4)_3SnX$ (X = F or OH) for comparison with previous mesityl (2,4,6-trimethylphenyl)- and phenyltin analogues.

The $(o\text{-}MeOC_6H_4)_3SnX$ structures (X = I [11] or NCS [8]) reported earlier show intramolecular $d(Sn\cdots O)$ values much less than van der Waals which are suggestive of increased coordination at tin. In addition the shortest Sn···O interaction is approximately *trans* to the Sn–X bond and the resulting geometry around tin resembles, to some extent, that found in the five-coordinate (2-carbomethoxy-1,4-cyclohexadien-1-yl)-dimethyltin halides (X = F, Cl, Br, I) [12]. However, in this series of compounds, a detailed comparison of the structure of the fluoride with those of the other halides provided evidence for an intermolecular Sn···F bond,

☆ For Part XIII; see Ref. [1].

* Corresponding author.

E-mail address: wharf@chemistry.mcgill.ca (I. Wharf)

0020-1693/99/$ - see front matter

PII: S0020-1693(99)00342-4

which although borderline to van der Waals (3.64 Å) and thus stretching the concept of a 'bonding interaction', was considered sufficient for the fluoride to be taken as a dimer with six-coordinate tin atoms. Thus, to make a similar comparison in this work, the crystal structures of both $(o\text{-MeOC}_6\text{H}_4)_3\text{SnF}$ and $(o\text{-MeOC}_6\text{H}_4)_3\text{SnCl}$ were determined.

The interconversion $(\text{Ar}_3\text{Sn})_2\text{O} \rightleftarrows \text{Ar}_3\text{SnOH}$ is facile when the Ar_3Sn moiety can readily achieve a five-coordinate *trans*-C_3SnZY trigonal-bipyramidal geometry at tin [1,13] and thus form a polymer structure like that of Ph_3SnOH [6]. This does not occur however when the aryl groups provide more steric hindrance at tin as is found with Ar = *o*-Tol, where there is no sign of hydroxide formation [1]. Here the effect of using Ar = *o*-Anis (*o*-Anis = *o*-MeOC_6H_4) as a sterically demanding aryl group on the above interconversion will be considered and the structure of the corresponding oxide is reported for comparison with other $(\text{Ar}_3\text{Sn})_2\text{O}$ (Ar = Ph [14] or *o*-Tol [15]) structures.

2. Experimental

All experimental details, including drying of solvents, synthetic procedures, microanalyses and spectroscopic methods (IR and both solution (CDCl_3) and solid-state NMR (^{119}Sn, ^{13}C)) were as given earlier [16–18]. *N*,*N*-Dimethylformamide (DMF) was dried by refluxing over CaH_2 while potassium fluoride was heated in vacuo until free-running before use. Tris(*o*-anisyl)tin iodide (**I**) and chloride (**A**), both recrystallised from ethanol, were previous preparations [19] as was tris(*o*-tolyl)tin oxide [1]; $(\text{Mes})_3\text{SnOH}$ and $(\text{Mes})_3\text{SnF}$ (Mes = 2,4,6-$\text{Me}_3\text{C}_6\text{H}_2$) were obtained using the literature procedure [7].

2.1. Synthesis

2.1.1. Fluorotris(o-methoxyphenyl)tin(IV) (B)

A yellow solution of **I** (2.56 g) in DMF (20 ml) was added under N_2 to a slurry of potassium fluoride (3.0 g) in DMF (25 ml). The colourless solution formed was stirred at room temperature for 48 h and then evaporated to dryness under vacuum. The residue was stirred with water, filtered, washed with ether and dried in vacuo; more product was obtained by adding water to the filtrate. Recrystallisation of the crude product from ethanol gave colourless crystals. Yield: 46%; m.p. 142–143°C. IR (mull), ν(Sn–F): 537 cm^{-1}. *Anal.* Calc. for $\text{C}_{21}\text{H}_{21}\text{FO}_3\text{Sn}$: C, 54.94; H, 4.61. Found: C, 55.25; H, 4.86%.

2.1.2. μ-Oxo-bis[tris(o-methoxyphenyl)tin(IV)] (C)

A mixture of **I** (1.40 g) in acetone (50 ml) and potassium hydroxide (5.3 g) in water (5 ml) was refluxed for 24 h and then evaporated under reduced pressure until only water was left. The white solid obtained on stirring the cooled mixture with methanol was filtered, washed with cold ethanol, and then recrystallised from CDCl_3–ethanol (1:4) to give the oxide. Yield: 45%; m.p. 143°C. IR (mull), ν_{as}(SnOSn): 853 cm^{-1}. *Anal.* Calc. for $\text{C}_{42}\text{H}_{42}\text{O}_7\text{Sn}_2$: C, 56.29; H, 4.72. Found: C, 56.56; H, 4.72%. Crystals for X-ray analysis were obtained by *slow* cooling of a hot DMF solution of **C**.

2.2. Crystal structure determinations

2.2.1. Data collection

For each compound a suitable crystal was selected from those available and X-ray data were collected ($T = 293(2)$ K) on a Rigaku AFC6S diffractometer. Cell measurements were by standard methods. For each compound, three standard reflections, measured every 250–150 reflections, showed 0.8–1.6% intensity decay over the data collection period for **A**–**C**, respectively. Full crystal parameters and data collection information are listed in Table 1.

2.2.2. Structure solution and refinement

The structures were solved by direct methods with SHELXS-96 [20] and difference maps using SHELXL-96 [21]. For **B**, the absolute structure was confirmed by the Flack parameter value of 0.036(14) [22]. All non-hydrogen atoms were anisotropic with H-atoms isotropic and calculated at idealised positions using a riding model, d(C–H) 0.93–0.98 Å; for each methyl hydrogen, U_{iso} was set at 50% greater than U_{iso} for its adjacent carbon atom, while all other U_{iso}(H) values were at $1.20 \times U_{iso}$(C). Neutral atom scattering factors were from the International Tables for Crystallography [23]. Further solution and refinement details are in Table 1. Selected geometric parameters and dihedral angles are reported in Tables 2 and 3, respectively. ORTEP [24] views of the molecules of **B** and **C** are shown in Figs. 1 and 2, respectively.

3. Results and discussion

3.1. Tris(o-methoxyphenyl)tin fluoride and chloride

Attempting to prepare $(o\text{-Anis})_3\text{SnF}$ using the procedure given for trimesityltin fluoride [7] i.e. by reacting tris(*o*-anisyl)tin iodide with KF in aqueous acetone always gave the crude oxide–hydroxide mixture (vide infra), presumably obtained from OH^- formed by reaction of F^- with the water present. Therefore, $(o\text{-Anis})_3\text{SnF}$ was prepared using dry DMF, an aprotic medium where any trace OH^- that might be formed would also be a weaker nucleophile than the fluoride

Table 1
Crystal parameters, and data collection and structure refinement information

	A	B	C
Formula	$C_{21}H_{21}ClO_3Sn$	$C_{21}H_{21}FO_3Sn$	$C_{42}H_{42}O_7Sn_2$
Formula mass	475.56	459.11	896.21
Crystal system	monoclinic	monoclinic	triclinic
Space group	$P2_1/n$	$P2_1$	$P\bar{1}$
Cell constants			
a (Å)	8.412(2)	8.332(3)	12.124(6)
b (Å)	27.755(5)	7.9309(13)	14.811(8)
c (Å)	8.987(10)	15.562(3)	12.000(3)
α (°)			91.44(4)
β (°)	97.18(4)	104.44(2)	107.64(3)
γ (°)			106.48(4)
V (Å^3)	2082(2)	995.8(4)	1954.7(15)
Z; D_{calc} (g cm^{-1})	4; 1.517	2; 1.531	2; 1.523
Crystal size (mm)	$0.92\times0.25\times0.05$	$0.46\times0.11\times0.05$	$0.47\times0.20\times0.20$
μ (mm^{-1})	1.376	10.462	1.326
Radiation (λ, Å)	Mo Kα_1 (0.70930)	Cu Kα_1 (1.54056)	Mo Kα_1 (0.71069)
Transmission range	0.84–0.96 (psi-scans)	0.05–0.19 (psi-scans)	0.69–1.00 (psi-scans)
Data collection method	ω scans	$\omega/2\theta$ scans	$\omega/2\theta$ scans
θ_{min}; θ_{max} (°)	2.4; 26.0	2.9; 60	2.7; 24.0
h, k, l ranges	$-10\rightarrow10$, $0\rightarrow34$, $-11\rightarrow11$	$-9\rightarrow+9$, $-9\rightarrow9$, $-18\rightarrow18$	$0\rightarrow14$, $-18\rightarrow18$, $-14\rightarrow14$
F(000)	952	460	900
No. reflections measured	8231	6314	6460
No. unique reflections	4092	2949	6133
No. observed reflections [$I\geq2\sigma(I)$]	2897	2691	4144
R_{int}	0.079	0.061	0.033
No. of parameters	239	239	467
R_1 [a] observed (total)	0.073 (0.117)	0.041 (0.047)	0.047 (0.092)
wR_2 observed (total)	0.190 (0.215)	0.090 (0.094)	0.103 (0.119)
Goodness-of-fit (S)	1.134	1.066	0.982
$\Delta\rho_{max}$ ($\Delta\rho_{min}$) (e Å^{-3})	1.349 (−1.505)	0.603 (−0.637)	0.727 (−0.845)

[a] $R_1=\Sigma(||F_o|-|F_c||)/\Sigma|F_o|$. $wR_2=\Sigma[w(F_o^2-F_c^2)^2/\Sigma(wF_o^2)^2]^{0.5}$. $S=\Sigma[w(F_o^2-F_c^2)^2/(\text{no. of reflections}-\text{no. of parameters})]^{0.5}$. Function minimised, $\Sigma[w(F_o^2-F_c^2]$.

ions present. While the formation of polymeric R_3SnF (R = Ph, *o*-Tol, alkyl) in aqueous alcohol media [25,26] must in large part be due to their very low solubilities, the factors governing the preparation of monomeric Ar_3SnF are clearly more subtle. However, once isolated, (*o*-Anis)$_3$SnF can be obtained unchanged from protic media such as water or ethanol showing the Sn–F bond, once formed, is stable to protic solvolysis.

IR data [ν(Sn–F)] suggest that (*o*-Anis)$_3$SnF is monomeric like (Mes)$_3$SnF (536 cm^{-1}) [7]. This conclusion is further supported by the very similar solid-state and solution NMR results for each compound (Table 4(a)). However, unlike the mesityl case, the ^{119}Sn NMR spectrum of solid (*o*-Anis)$_3$SnF consists of one doublet caused by coupling to a single fluorine, indicating only one molecule per asymmetric unit.

X-ray analysis of (*o*-Anis)$_3$SnF (**B**) confirms that it is indeed monomeric with the shortest intermolecular Sn···F distance being 6.865 Å. The arrangement of *o*-anisyl groups around tin (Fig. 1) is the same as that found for the isothiocyanate [8], the chloride (**A**) and the iodide (**I**) [11]. This motif has one $CH_3O(2)$ *trans* and the other two methoxy groups (1) and (3), *cis* to the Sn–X bond with phenyl ring (2) almost coplanar with the C(21)–Sn–X unit [Table 3(a,b)]. However, while detailed structures of **A** and **I** are almost identical, the SnC_3X unit in **B** is more distorted from trigonal symmetry and the *trans* O(2)···Sn–X angle distinctly smaller, when compared with **A** or **I** [Table 2(a,b)]. This change may be due to the increased interaction between X and O(1) and O(3) in **B** which will occur with the flattening of the SnC_3 unit on going from **A** to **B**.

Detailed comparison of *ortho*-substituted Ar_3SnX structures with those of analogous Ph_3SnX would be unwieldy but the results of a simpler procedure are shown in Table 5. The change in angle sums, $\Sigma\theta_{ax}=\Sigma\angle CSnX$ (°) and $\Sigma\theta_{eq}=\Sigma\angle CSnC$ (°) [12] is equivalent to that used earlier to assess changes in the central tin atom environment in various triaryltin pseudohalide structures [8,18]. Even in cases where averaged data are given, errors are less than ±2 in $\Sigma\theta_{ax}$ and $\Sigma\theta_{eq}$, so the changes observed, although small, are real.

All Ph_3SnX show almost the same distortion from inner tetrahedral geometry with $\Sigma\theta_{eq}>\Sigma\theta_{ax}$. However,

Table 2
Selected geometric parameters (Å, °)

*(a) Chlorotris(o-methoxyphenyl)tin(IV) (**A**)*			
Sn–Cl	2.371(5)	Sn–C(11)	2.129(11)
Sn–C(21)	2.129(12)	Sn–C(31)	2.105(13)
O(1)–C(16)	1.361(14)	O(1)–C(17)	1.438(14)
O(2)–C(26)	1.38(2)	O(2)–C(27)	1.42(2)
O(3)–C(36)	1.36(2)	O(3)–C(37)	1.44(2)
Sn···O(1)	3.090(9)	Sn···O(2)	2.974(10)
Sn···O(3)	3.061(11)	Cl···O(1)	3.534(10)
Cl···O(2)	5.180(10)	Cl···O(3)	3.676(10)
C(11)–Sn–Cl	110.3(3)	C(21)–Sn–Cl	100.9(3)
C(31)–Sn–Cl	106.6(4)	C(11)–Sn–C(21)	113.5(4)
C(21)–Sn–C(31)	112.0(5)	C(11)–Sn–C(31)	112.8(5)
Sn–C(11)–C(12)	118.7(8)	Sn–C(11)–C(16)	119.7(8)
Sn–C(21)–C(22)	124.5(9)	Sn–C(21)–C(26)	116.8(9)
Sn–C(31)–C(32)	121.8(11)	Sn–C(31)–C(36)	120.4(10)
C(16)–O(1)–C(17)	118.4(10)	C(26)–O(2)–C(27)	119.3(12)
C(36)–O(3)–C(37)	118.3(13)	O(1)–C(16)–C(11)	116.3(10)
O(1)–C(16)–C(15)	123.7(11)	O(2)–C(26)–C(21)	113.4(11)
O(2)–C(26)–C(25)	125.2(12)	O(3)–C(36)–C(31)	113.8(11)
O(3)–C(36)–C(35)	124(2)	O(1)···Sn–Cl	79.5(2)
O(2)···Sn–Cl	151.3(2)	O(3)···Sn–Cl	84.2(2)
*(b) Fluorotris(o-methoxyphenyl)tin(IV) (**B**)*			
Sn–F	1.972(5)	Sn–C(11)	2.112(8)
Sn–C(21)	2.120(9)	Sn–C(31)	2.129(8)
O(1)–C(16)	1.365(11)	O(1)–C(17)	1.432(14)
O(2)–C(26)	1.370(13)	O(2)–C(27)	1.423(11)
O(3)–C(36)	1.382(11)	O(3)–C(37)	1.426(12)
Sn···O(1)	3.088(8)	Sn···O(2)	3.026(8)
Sn···O(3)	3.108(7)	F···O(1)	3.456(10)
F···O(2)	4.806(10)	F···O(3)	3.333(10)
C(11)–Sn–F	104.9(3)	C(21)–Sn–F	98.4(3)
C(31)–Sn–F	106.5(3)	C(11)–Sn–C(21)	124.7(3)
C(21)–Sn–C(31)	107.9(3)	C(11)–Sn–C(31)	112.2(3)
Sn–C(11)–C(12)	121.0(6)	Sn–C(11)–C(16)	119.8(8)
Sn–C(21)–C(22)	121.6(7)	Sn–C(21)–C(26)	119.0(7)
Sn–C(31)–C(32)	120.9(6)	Sn–C(31)–C(36)	120.7(6)
C(16)–O(1)–C(17)	117.4(13)	C(26)–O(2)–C(27)	118.1(9)
C(36)–O(3)–C(37)	118.4(8)	O(1)–C(16)–C(11)	115.0(13)
O(1)–C(16)–C(15)	124.7(14)	O(2)–C(26)–C(21)	114.2(10)
O(2)–C(26)–C(25)	125.0(10)	O(3)–C(36)–C(31)	115.6(7)
O(3)–C(36)–C(35)	122.4(9)	O(1)···Sn–F	83.0(3)
O(2)···Sn–F	147.2(3)	O(3)···Sn–F	78.5(2)
*(c) Oxobis[tris(o-methoxyphenyl)tin(IV)] (**C**)*			
Sn(1)–O(1)	1.940(5)	Sn(2)–O(1)	1.915(5)
Sn(1)–C(11)	2.136(7)	Sn(2)–C(41)	2.143(8)
Sn(1)–C(21)	2.133(7)	Sn(2)–C(51)	2.111(8)
Sn(1)–C(31)	2.128(7)	Sn(2)–C(61)	2.141(7)
O(11)–C(16)	1.344(10)	O(41)–C(46)	1.372(9)
O(11)–C(17)	1.418(10)	O(41)–C(47)	1.414(9)
O(21)–C(26)	1.368(9)	O(51)–C(56)	1.375(9)
O(21)–C(27)	1.427(10)	O(51)–C(57)	1.432(10)
O(31)–C(36)	1.374(10)	O(61)–C(66)	1.364(9)
O(31)–C(37)	1.414(10)	O(61)–C(67)	1.435(9)
Sn(1)···O(11)	3.127(7)	Sn(2)···O(41)	3.052(6)
Sn(1)···O(21)	3.119(7)	Sn(2)···O(51)	3.057(7)
Sn(1)···O(31)	3.133(6)	Sn(2)···O(61)	3.117(5)
O(1)···O(41)	3.260(8)	O(1)···O(51)	3.398(9)
O(31)···O(11)	3.100(11)	O(31)···O(21)	3.096(9)
C(11)–Sn(1)–O(1)	99.7(3)	C(41)–Sn(2)–O(1)	104.5(3)
C(21)–Sn(1)–O(1)	102.4(3)	C(51)–Sn(2)–O(1)	112.3(3)
C(31)–Sn(1)–O(1)	105.9(3)	C(61)–Sn(2)–O(1)	99.9(3)
C(11)–Sn–C(21)	109.9(3)	C(41)–Sn–C(51)	110.7(3)
C(21)–Sn–C(31)	118.6(3)	C(51)–Sn–C(61)	118.0(3)
C(11)–Sn–C(31)	117.3(3)	C(41)–Sn–C(61)	110.2(3)
Sn(1)–C(11)–C(12)	119.2(6)	Sn(2)–C(41)–C(42)	123.5(6)
Sn(1)–C(11)–C(16)	121.8(6)	Sn(2)–C(41)–C(46)	118.0(6)
Sn(1)–C(21)–C(22)	120.3(6)	Sn(2)–C(51)–C(52)	123.0(6)
Sn(1)–C(21)–C(26)	121.0(6)	Sn(2)–C(51)–C(56)	119.2(6)
Sn(1)–C(31)–C(32)	120.6(6)	Sn(2)–C(61)–C(62)	119.7(5)
Sn(1)–C(31)–C(36)	121.3(6)	Sn(2)–C(61)–C(66)	120.7(5)
C(16)–O(11)–C(17)	120.1(8)	C(46)–O(41)–C(47)	119.2(7)
C(26)–O(21)–C(27)	119.9(7)	C(56)–O(51)–C(57)	120.2(7)
C(36)–O(31)–C(37)	120.3(8)	C(66)–O(61)–C(67)	117.9(6)
O(11)–C(16)–C(11)	114.8(7)	O(41)–C(46)–C(41)	115.1(7)
O(11)–C(16)–C(15)	124.3(8)	O(41)–C(46)–C(45)	123.9(7)
O(21)–C(26)–C(21)	115.5(7)	O(51)–C(56)–C(51)	115.5(7)
O(21)–C(26)–C(25)	123.5(8)	O(51)–C(56)–C(55)	121.6(8)
O(31)–C(36)–C(31)	115.3(7)	O(61)–C(66)–C(61)	115.3(6)
O(31)–C(36)–C(33)	122.5(9)	O(61)–C(66)–C(65)	123.6(7)
O(11)···Sn(1)–O(1)	145.8(2)	O(41)···Sn(2)–O(1)	78.4(2)
O(21)···Sn(1)–O(1)	102.3(2)	O(51)···Sn(2)–O(1)	82.8(2)
O(31)···Sn(1)–O(1)	149.7(2)	O(61)···Sn(2)–O(1)	147.9(20
Sn(1)–O–Sn(2)	167.0(4)		

the general trend is for the C_3Sn pyramid to steepen as Cl is replaced by Br and then I, presumably due to *o*-H···X interactions. Such intramolecular *ortho*-effects are of much greater import in $(Mes)_3SnX$ where the geometry around tin reflects the balance of repulsions between proximal *o*-CH_3 groups and interactions between distal *o*-CH_3 groups with the axial X atom. The result is for the C_3Sn pyramid to be flatter than in the Ph_3SnX case and an increase in *d*(Sn–I) [31]. At this time X-ray data for $(Mes)_3SnX$ (X = Cl, Br) are not available to show whether the small change in geometry around tin in going from the fluoride to the iodide is gradual over the series, or abrupt as F is replaced by Cl. This abrupt change however occurs in the *ortho*-anisyl series. Thus, **A** and **I** have effectively the same environment at tin which resembles that for Ph_3SnX. However, for **B**, $\Sigma\theta_{eq}$ and $\Sigma\theta_{ax}$ values differ significantly from those for **A** or **I**, resembling more those found for $(Mes)_3SnX$.

^{119}Sn NMR data for $(o\text{-Anis})_3SnX$, when compared with those for other Ar_3SnX (Ar = Ph or Mes) (Table 5), also indicate that the effects of *ortho*-substituents are not the same in the *ortho*-anisyl and mesityl series. All three Ar_3SnX series show the shift to higher frequency of $\delta(^{119})$ as X = I is replaced by more electronegative Br and then Cl, with $(Mes)_3SnF$ continuing this trend. Plotting $\delta(^{119}Sn)$ data for Ph_3SnX or $(o\text{-Anis})_3SnX$ versus $(Mes)_3SnX$, gives $\delta(Ph) = 0.525\,\delta(Mes) + 1.13$ ($r = 0.998$), and $\delta(o\text{-Anis}) = 0.603\,\delta(Mes) - 3.85$ ($r = 0.998$), respectively. Inserting the ^{119}Sn chemical shift for $(Mes)_3SnF$ then predicts $\delta(^{119}Sn)$ values of -33.8 ppm for the hypothetical Ph_3SnF monomer in solution but more significantly,

Table 3
Selected dihedral angles (°) [a]

(a) Chlorotris(o-methoxyphenyl)tin(IV) (A)		
(A) Cl–Sn–C(11)	Cl–Sn–C(21)	Cl–Sn–C(31)
(B) Phenyl ring (1)	Phenyl ring (2)	Phenyl ring (3)
54.9(4)	8.9(5)	68.0(5)
(b) Fluorotris(o-methoxyphenyl)tin(IV) (B)		
(A) F–Sn–C(11)	F–Sn–C(21)	F–Sn–C(31)
(B) Phenyl ring (1)	Phenyl ring (2)	Phenyl ring (3)
66.5(3)	8.4(4)	58.6(3)
(c) Oxobis[tris(o-methoxyphenyl)tin(IV)] (C)		
(A) O(1)–Sn(1)–C(11)	O(1)–Sn(1)–C(21)	O(1)–Sn(1)–C(31)
(B) Phenyl ring (1)	Phenyl ring (2)	Phenyl ring (3)
9.4(3)	82.5(3)	19.6(5)
(A) O(1)–Sn(2)–C(41)	O(1)–Sn(2)–C(51)	O(1)–Sn(2)–C(61)
(B) Phenyl ring (4)	Phenyl ring (5)	Phenyl ring (6)
59.1(3)	59.2(3)	3.7(3)

[a] Angle between planes (A) and (B).

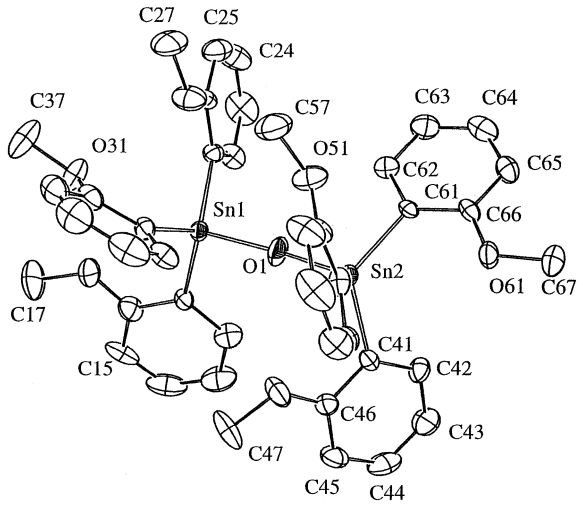

Fig. 2. ORTEP view of the molecule of **C** showing the numbering scheme adopted. Ellipsoids are drawn at 40% probability level.

-44.0 ppm for $(o\text{-Anis})_3SnF$. The $\delta(^{119}Sn)$ values of $(o\text{-Anis})_3SnX$ (X = Cl, Br, I) and $(o\text{-Anis})_4Sn$ are more negative compared with the phenyltin data [19], perhaps due to weak Sn···O interactions increasing shielding at tin since there is little structural change on going from a phenyl compound to its *o*-anisyl analogue. However, $\delta(^{119}Sn)$ for the fluoride is at much lower frequency than expected on this basis and this appears to coincide with the abrupt flattening of the C_3Sn pyramid in going from $(o\text{-Anis})_3SnCl$ to $(o\text{-Anis})_3SnF$. A similar large shift to low frequency for $\delta(^{119}Sn)$ of $(Mes)_3SnI$ compared with Ph_3SnI was also earlier correlated with the opening up of the CSnC angles around tin [19]. For the trimesityltin system this is mainly due to the steric crowding of the *ortho*-methyl groups. For $(o\text{-Anis})_3SnX$, since flattening of the C_3Sn pyramid as X = Cl is replaced by F increases the steric strain in the molecule, it is more likely due to the high greater ionic character of the Sn–F bond causing an increase in s-character of the Sn–C bonds with the accompanying opening out of the CSnC angles. However, while such correlations of trends in solution ^{119}Sn data with solid-state structural changes must be viewed as speculative, the close similarity of solution and solid-state ^{119}Sn data for both $(o\text{-Anis})_3SnF$ and $(Mes)_3SnF$ would suggest the same structural features are responsible for the NMR trends in both $CDCl_3$ solution and the solid-state. Solid-state ^{119}Sn NMR studies of a wide range of Ar_3SnX (X = Cl, Br) are now in progress for comparison with data from earlier solution studies [16,19].

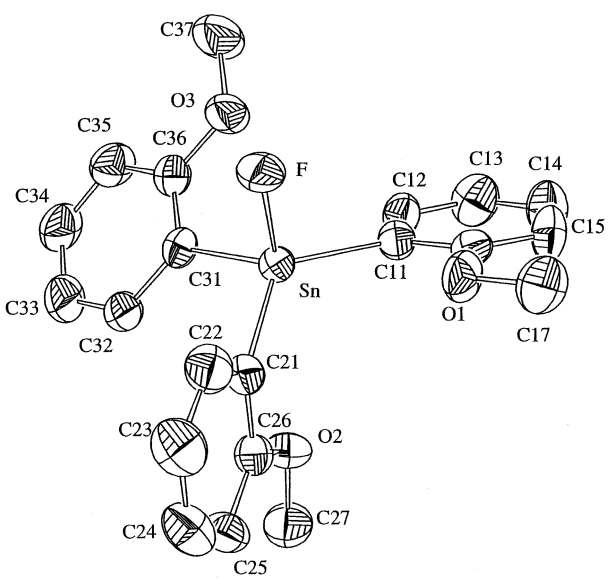

Fig. 1. ORTEP view of the molecule of **B** showing the numbering scheme adopted. Ellipsoids are drawn at 40% probability level. The same numbering scheme was also used for molecule **A**.

3.2. Tris(o-methoxyphenyl)tin oxide and hydroxide

All freshly prepared samples of '$(o\text{-Anis})_3SnOH$' gave two peaks in the ^{119}Sn spectrum ($CDCl_3$ solution) at -83 and -98 ppm, the latter usually predominant. Saturating one of these solutions with water eliminated the lower frequency peak, thus allowing the peak at -83 ppm to be assigned to the hydroxide [Table 4(b)]. Recrystallising the crude '$(o\text{-Anis})_3SnOH$' from ethanol or ethanol/$CDCl_3$ gave the OH-free oxide (IR), confirmed by the single ^{119}Sn resonance at -98 ppm with satellites due to $^{119}Sn-^{117}Sn$ spin coupling, observed in $CDCl_3$ solution [Table 4(b)]. Indeed, the almost complete loss of OH from '$(o\text{-Anis})_3SnOH$' samples occurs at room temperature simply by more rigorous drying in vacuum or leaving them open to the atmosphere overnight. This behaviour means, as found earlier for $(neophyl)_3SnOH$ [34], that $(o\text{-Anis})_3SnOH$ can not be isolated and may only be identified in solution.

Table 4
Solution ($CDCl_3$) and solid-state NMR data [a] for Ar_3SnX

(a) X = F	Ar =	*o*-Anis		Mes			
		Solution	Solid	Solution	Solid [b]		
$\delta(^{119}Sn)$ ppm		−74.05	−77.10	−66.51	−70.6, −82.2		
$^1J(^{119}Sn–^{13}C)$ Hz		714.6		625.7			
$^1J(^{119}Sn–^{19}F)$ Hz		2286.5	2240.0	2285.5	2300, 2256		
$^2J(^{19}F–^{13}C)$ Hz		12.7		9.9			
(b)		X = 1/2O				X = OH	
	Ar =	*o*-Anis		*o*-Tol		*o*-Anis [c]	Mes[d]
		Solution	Solid	Solution [d]	Solid	Solution	Solution
$\delta(^{119}Sn)$ ppm		−98.42	−93.26, −109.76	−77.20	−54.08	−83.12	−101.78
$^1J(^{119}Sn–^{13}C)$ Hz		660.2		617.1		679.3	614.7
$^2J(^{119}Sn–^{119}Sn)$ Hz		471.2	650.6	576.1	801.6		

[a] [Sn] = 0.2–0.4 M; Ref: (^{119}Sn), ext. $(CH_3)_4Sn$; (^{13}C), int. $(CH_3)_4Si$.
[b] Ref [27].
[c] $CDCl_3$ solution of $[(o\text{-Anis})_3Sn]_2O$ saturated with water.
[d] Ref. [1].

IR data [ν_{as}(SnOSn)] indicated that $[(o\text{-Anis})_3Sn]_2O$ (**C**) in the solid state might be more like linear $[(o\text{-Tol})_3Sn]_2O$ (839 cm^{-1}) [1,15] rather than angular $(Ph_3Sn)_2O$ (776 cm^{-1}) [13,14]. However, the solid-state ^{119}Sn NMR spectrum of the *o*-anisyltin system shows that there are in fact two distinct tin environments in contrast to the single peak observed with symmetric $[(o\text{-Tol})_3Sn]_2$ [Table 4(b)]. Furthermore, from the correlation of $^2J(^{119}Sn,^{119}Sn)$ with molecular structure given by Lockhart et al. [15], we can predict that **C** would be the first distannoxane with an Sn–O–Sn angle between 140 and 180°.

The X-ray diffraction study of **C** confirms these predictions, the molecule (Fig. 2) having two quite different geometries around each tin and a bent Sn–O–Sn skeleton (167°). The architecture of *o*-anisyl

Table 5
Comparison of tin atom environments with solution ($CDCl_3$) NMR results for various Ar_3SnX complexes

Ar_3SnX		Geometric parameters [a]				NMR data [b]	
Ar	X	*d*(Sn–X) (Å)	$\Sigma\theta_{ax}$ [c]	$\Sigma\theta_{eq}$ [c]	$(\Sigma\theta_{eq}-\Sigma\theta_{ax})$	$\delta(^{119}Sn)$ (ppm)	$^1J(^{119}Sn–^{13}C)$ (Hz)
Ph	Cl [d]	2.360	314	341	27	−44.81	615.7
	Br [e]	2.495	316	340	24	−60.01	596.3
	I [f]	2.704	319	337	18	−113.38	570.9
o-Anis	F	1.972	310	345	35	−74.05	714.6
	Cl	2.371	318	338	20	−56.68	684.8
	Br					−74.31	666.2
	I [g]	2.713	318	338	20	−135.65	635.8
Mes	F [h]	1.961	303	349	46	−66.51	625.7
	Cl					−84.39	596.1
	Br					−120.98	579.8
	I [i]	2.750	308	346	38	−217.10	554.0

[a] Averaged values when two or more data sets are available.
[b] This work or Ref. [19].
[c] $\Sigma\theta_{ax} = \Sigma\angle$CSnX (°), $\Sigma\theta_{eq} = \Sigma\angle$CSnC(°).
[d] Ref. [28,29].
[e] Ref. [30].
[f] Ref. [31,32].
[g] Ref. [11].
[h] Ref. [7].
[i] Ref. [31].

Table 6
Correlation of ^{119}Sn NMR data with structural parameters for various $(Ar_3Sn)_2O$ complexes

(a) ^{119}Sn NMR data						
Ar	$\delta(^{119}Sn)$ (ppm)		$^2J(^{119}Sn–^{119}Sn)$ (Hz)			
	$CDCl_3$	Solid	$CDCl_3$	Solid		
Ph	−83.47 [a] −80.5	−75.2 [b]	410.8 [a]	421 [b]		
o-Anis	−98.42 −109.76	−93.26	471.2	650.6		
o-Tol	−77.20 [a]	−54.08	576.1 [a]	801.6		
(b) Structural parameters						
Ar	Sn	d(Sn–O) (Å)	∠SnOSn (°)	$\Sigma\theta_{ax}$ [c]	$\Sigma\theta_{eq}$ [c]	$(\Sigma\theta_{eq}-\Sigma\theta_{ax})$
Ph [d]	(1)	1.957	137.3	315	340	25
	(2)	1.953		320	336	16
o-Anis	(1)	1.940	167.0	308	346	38
	(2)	1.915		317	337	20
o-Tol [e]		1.922	180.0	323	333	10

[a] Ref. [1].
[b] Ref. [33].
[c] $\Sigma\theta_{ax} = \Sigma\angle$CSnO (°), $\Sigma\theta_{eq} = \Sigma\angle$CSnC (°).
[d] Ref. [14].
[e] Ref. [15].

groups around Sn(2) is almost the same as that found for **A** and **B**, having one $CH_3O(6)$ *trans* and the other two methoxy groups (4) and (5) *cis* to the Sn(2)–O bond [Table 2(c)] with phenyl ring (6) almost coplanar with the C(61)–Sn–O(1) unit [Table 3(c)]. In contrast, for Sn(1) all three methoxy groups are *trans* to the Sn(1)–O bond, presumably to lessen interatomic repulsions between the two $(o\text{-Anis})_3Sn$ units.

Correlation of solid-state ^{119}Sn NMR data with structural parameters (Table 6) for the three $(Ar_3Sn)_2O$ (Ar = Ph, *o*-Anis, *o*-Tol) gives $\angle SnOSn = 0.114\ ^2J(^{119}Sn,^{119}Sn) + 89.93$; $r = 0.995$. Inserting $CDCl_3$ solution $^2J(^{119}Sn,^{119}Sn)$ values in the equation then indicates Sn–O–Sn angles, in solution, of 137, 144, and 156° for the given $(Ar_3Sn)_2O$ species, Ar = Ph, *o*-Anis, *o*-Tol, respectively. Thus, for $[(o\text{-Anis})_3Sn]_2O$ as was found earlier for two hexabenzyldistannoxanes [15], it is the change in the ^2J value and not the chemical shift which suggests a structural change occurs on going from the solid state to the solution. However, for $[(o\text{-Tol})_3Sn]_2O$, both NMR parameters are affected when the sample is dissolved with the Sn–O–Sn skeleton changing from linear to bent. In addition our data do not show the previously reported considerable high field shift of the tin resonance of $[(o\text{-Tol})_3Sn]_2O$ [15].

Inspection of tin atom environments [$\Sigma\theta_{ax}$, $\Sigma\theta_{eq}$, $(\Sigma\theta_{eq} - \Sigma\theta_{ax})$] in the three $(Ar_3Sn)_2O$ (Ar = Ph, *o*-Anis, *o*-Tol) [Table 6(b)] provides more evidence of the special nature of the hexakis-(*o*-tolyl)distannoxane structure in the solid state. Thus, for both $(Ph_3Sn)_2O$ and $[(o\text{-Anis})_3Sn]_2O$, $\Sigma\theta_{ax}$ and $\Sigma\theta_{eq}$ values are comparable with those found in the corresponding triaryltin halides (Table 5), but for the tris(*o*-tolyl)tin oxide, $\Sigma\theta_{ax} = 323$ and $\Sigma\theta_{eq} = 333$ are unexpectedly close to the 'ideal' tetrahedral value, $\Sigma\theta_{ax} = \Sigma\theta_{eq} = 328°$. In contrast, the geometries around the two atoms tin in $(o\text{-Tol})_3SnNCS$ ($\Sigma\theta_{ax} = 314°$, $\Sigma\theta_{eq} = 342°$; $\Sigma\theta_{ax} = 311°$, $\Sigma\theta_{eq} = 344°$) are similar to that found in $(o\text{-Anis})_3SnNCS$ ($\Sigma\theta_{ax} = 315°$, $\Sigma\theta_{eq} = 333°$) [8] which itself is between the tin geometries determined for the corresponding chloride **A** and fluoride **B** (Table 5).

The factors which determine the amplitude of the M–O–M angle in $(R_3M)_2O$ (M = C–Pb) are as yet unresolved. These include the relative ground state (linear or bent) energies of the molecule, the consequences of intramolecular interactions between the two end R_3M units, as well as crystal packing effects in the solid state. Several years ago Glidewell [35] argued that electronic rather than steric factors would predominate, and could account for the change in geometry from angular $(Ph_3C)_2O$ [36] to linear $(Ph_3Si)_2O$ [37] which has the same symmetric structure as $[(o\text{-Tol})_3Sn]_2O$ [15]. However, in contradiction, both $(Ph_3Ge)_2O$ [38] and $(Ph_3Sn)_2O$ [14] have bent M–O–M skeletons, leading to the conclusion that in these systems a large amplitude bending vibration can occur, meaning that it is characteristic of $(R_3M)_2O$ that the M–O–M angle may be markedly changed with the expenditure of very little energy. In this case, crystal packing effects then can stabilise one molecular shape over the another. Our

results, together with those of Lockhart et al. [15], indicate that $(R_3Sn)_2O$ structures with larger Sn–O–Sn angles are more favoured in the solid state. Thus, crystal packing effects are significant in determining the size of the Sn–O–Sn angle while both linear and bent $R_3Sn–O–SnR_3$ structures have very similar energies.

Acknowledgements

The financial assistance of the 'Fonds FCAR (programme Soutien aux Équipes de Recherche)' of the 'Gouvernement du Québec' is most gratefully acknowledged. We also thank Dr Céline Pearson for carrying out the X-ray structure determination of compound **A**. The authorities of Dawson College, Montreal, are also thanked for providing release time, thus enabling this research to be carried out.

References

[1] I. Wharf, Appl. Organomet. Chem. (1999) in press.
[2] I. Wharf, A.-M. Lebuis, H. Lamparski, Acta Crystallogr., Sect. C 52 (1996) 2477 and Refs. therein.
[3] I. Wharf, A.-M. Lebuis, Acta Crystallogr., Sect. C 52 (1996) 3025.
[4] I. Wharf, M.G. Simard, J. Organomet. Chem. 532 (1974) 1.
[5] D. Tudela, E. Gutierrez-Puebla, A. Monge, J. Chem. Soc., Dalton Trans. (1992) 1069.
[6] C. Glidewell, D.C. Liles, Acta Crystallogr., Sect. B 34 (1978) 129.
[7] H. Reuter, H. Puff, J. Organomet. Chem. 379 (1989) 223.
[8] I. Wharf, M.G. Simard, Inorg. Chim. Acta 282 (1998) 30.
[9] A.M. Domingos, G.M. Sheldrick, J. Organomet. Chem. 67 (1974) 257.
[10] L.E. Khoo, X.-M. Chen, T.C. Mak, Acta Crystallogr., Sect. C 47 (1991) 2647.
[11] R.A. Howie, J.-N. Ross, J.L. Wardell, J.N. Low, Acta Crystallogr., Sect. C 50 (1994) 229.
[12] U. Kolb, M. Dräger, B. Jousseaume, Organometallics 10 (1991) 2737.
[13] I. Wharf, H. Lamparski, R. Reeleder, Appl. Organomet. Chem. 11 (1997) 969.
[14] C. Glidewell, D.C. Liles, Acta Crystallogr., Sect. B 34 (1978) 1693.
[15] T.P. Lockhart, H. Puff, W. Schluh, H. Reuter, T.N. Mitchell, J. Organomet. Chem. 366 (1989) 61.
[16] I. Wharf, Inorg. Chim. Acta 159 (1989) 41.
[17] I. Wharf, A. Bastone, E.J. Bures, Can. J. Spectrosc. 41 (1996) 122.
[18] I. Wharf, R. Wojtowski, C. Bowes, A.-M. Lebuis, M. Onyszchuk, Can. J. Chem. 76 (1998) 1827.
[19] I. Wharf, M.G. Simard, J. Organomet. Chem. 532 (1997) 1.
[20] G.M. Sheldrick, SHELXS-96, Program for the solution of crystal structures, University of Göttingen, Germany, 1996.
[21] G.M. Sheldrick, SHELXL-96, Program for structure analysis, University of Göttingen, Germany, 1996.
[22] H.D. Flack, Acta Crystallogr., Sect. A 39 (1983) 876.
[23] International Tables for Crystallography, vol. C, Kluwer, Dordrecht, Holland, 1992, Tables 4.2.6.
[24] C.K. Johnson, ORTEPII, Rep. ORNL-5138, Oak Ridge National Laboratory, TN, USA, 1976.
[25] E. Krause, R. Becker, Chem. Ber. 53 (1926) 173.
[26] D. Tudela, R. Fernandez, V.K. Belsky, V.E. Zavodnik, J. Chem. Soc., Dalton Trans. (1996) 2123.
[27] H. Bai, R.K. Harris, H. Reuter, J. Organomet. Chem. 408 (1991) 167.
[28] J.S. Tse, F.L. Lee, E.J. Gabe, Acta Crystallogr., Sect. C 42 (1986) 1876.
[29] S.W. Ng, Acta Crystallogr., Sect. C 51 (1995) 2292.
[30] H. Preut, F. Huber, Acta Crystallogr., Sect. B 35 (1979) 2292.
[31] M.G. Simard, I. Wharf, Acta Crystallogr., Sect. C 50 (1994) 397.
[32] S.W. Ng, Acta Crystallogr., Sect. C 51 (1995) 629.
[33] R.K. Harris, A. Sebald, Magn. Res. Chem. 27 (1989) 81.
[34] T.P. Lockhart, J. Organomet. Chem. 287 (1989) 179.
[35] C. Glidewell, J. Organomet. Chem. 159 (1978) 23.
[36] C. Glidewell, D.C. Liles, Acta Crystallogr., Sect. B 34 (1978) 696.
[37] C. Glidewell, D.C. Liles, Acta Crystallogr., Sect. B 34 (1978) 124.
[38] C. Glidewell, D.C. Liles, Acta Crystallogr., Sect. B 34 (1978) 119.